Journal of Applied Physics

Host–guest exchange contribution to transition temperature downshift in nanocrystalline Fe(pyrazine)[Pt(CN)$_4$] thin films prepared by matrix-assisted pulsed laser evaporation

Cite as: J. Appl. Phys. **129**, 155308 (2021); https://doi.org/10.1063/5.0047749
Submitted: 16 February 2021 . Accepted: 29 March 2021 . Published Online: 21 April 2021

Mirosław Sawczak, Rafał Jendrzejewski, Dominik Maskowicz, Yann Garcia, Marinela Dîrtu, Varun Kumar, and Gerard Śliwiński

Journal of Applied Physics ARTICLE scitation.org/journal/jap

Host–guest exchange contribution to transition temperature downshift in nanocrystalline Fe(pyrazine)[Pt(CN)$_4$] thin films prepared by matrix-assisted pulsed laser evaporation

Cite as: J. Appl. Phys. **129**, 155308 (2021); doi: 10.1063/5.0047749
Submitted: 16 February 2021 · Accepted: 29 March 2021 ·
Published Online: 21 April 2021

Mirosław Sawczak,[1,a)] Rafał Jendrzejewski,[1] Dominik Maskowicz,[1] Yann Garcia,[2] Marinela Dîrtu,[3] Varun Kumar,[2] and Gerard Śliwiński[1]

AFFILIATIONS

[1]Institute of Fluid Flow Machinery, Polish Academy of Sciences, Photophysics Dept., 14 Fiszera St, 80-231 Gdańsk, Poland
[2]Institute of Condensed Matter and Nanosciences, Molecular Chemistry, Materials and Catalysis (IMCN/MOST), Université catholique de Louvain, Place L. Pasteur 1, 1348 Louvain-la-Neuve, Belgium
[3]Faculty of Electrical Engineering and Computer Science & MANSiD Research Center, Stefan cel Mare University, 720229 Suceava, Romania

Note: This paper is part of the Special Topic on Spin Transition Materials: Molecular and Solid-State.

[a)]**Author to whom correspondence should be addressed:** mireks@imp.gda.pl

ABSTRACT

The influence of guest molecules affecting the spin transition characteristics of iron(II) complexes represents a widely discussed topic because it opens the possibility of using this type of materials in many fields of science, especially if the material properties could be tuned in a controlled way. We report an experimental observation of the spin transition in thin films of a 3D Hoffman framework nanocrystalline material Fe(pyrazine)[Pt(CN)$_4$] deposited by nanosecond laser ablation at $\lambda = 1064$ nm of its cryo-cooled colloidal suspension in water and water-free organic solvents. For vacuum deposited films (thickness 120 nm), the substantial downshift in temperature, gradual spin transition, and shrinkage of the temperature hysteresis compared to the starting material are ascribed to incomplete removal of water molecules from the porous network and partial destruction of the crystalline site caused by laser heating. The destructive effect of laser irradiation occurring in vacuum conditions was not observed for deposition conducted in N_2 at atmospheric pressure. In this case, thin films reproducing properties of the reference material with transition temperature near 276 K and 12 K wide hysteresis were obtained. In addition, the changes in the spin switching characteristics associated with the exchange of guest molecules in the SCO crystal lattice were observed using a water-free solvent as a matrix for the laser based thin film deposition. The observed laser induced host–guest exchange indicates on the possibility of selective modification of thin layers of SCO materials to obtain their desired characteristics.

I. INTRODUCTION

The application capacity of the family of 3D Hoffman-like hybrid framework materials is seriously limited due to the fragility of the nanocrystalline framework and a relatively low vaporization temperature resulting in irreversible structural decomposition characteristic for most of the compounds, which are, therefore, considered non-sublimable.[1] This results in the inability of the controlled fabrication of thin films of a large collection of 3D framework materials,[2] which are well characterized at the research scale and can be produced mainly with the use of the chemical solution based methods. While these methods are well established, easily applicable, and their modifications are currently proposed,[3] they do not provide scalability and reproducibility required for the implementation of SCO materials into optoelectronic devices.[4] This stimulates not only the search on novel sublimable compounds but also studies on innovative approaches such as functional thin films

obtained by multilayer sequential assembly,[5] step-by-step approach,[6] or the $[Fe(HB(tz)_3)_2]$ (tz = 1,2,4-triazole) 120 nm thick high quality films obtained by vacuum evaporation combined with recrystallization and solvent–vapor annealing.[7] Recently, the application of the matrix assisted pulsed laser evaporation (MAPLE) for the deposition of SCO compounds has been reported.[8]

This method has been developed, in particular, for the deposition of fragile and vulnerable molecular materials of organic origin.[9] For deposition, the compound to be deposited is suspended and frozen at cryogenic temperature to serve as a target for pulsed laser ablation. The deposition proceeds by the immobilization of the ablated compound particles on the substrate at the instantaneous evacuation of the evaporated matrix material.

Successful thin film fabrication by means of MAPLE was observed for biological, organic, and hybrid molecules and complexes, also in the nanoparticle[10] form. In most cases, the deposition was controlled regarding the film thickness and porosity/continuity. An exceptionally low roughness down to about 10 nm was observed for light emitting polymer films of thickness of 40 nm as used in documented optoelectronic devices.[11]

In the case of the coordination polymer $RbMn[Fe(CN)_6]$, the MAPLE film fabrication was performed using nanoparticles (NPs) of the compound. The bimetal assembly has been selected due to the reported extremely attractive charge transfer-induced phase transition found useful for the switching property.[12] Indeed, the films of $RbMn[Fe(CN)_6]$ exhibited temperature-induced phase transition and bistability within a broad hysteresis loop of the width of 120 K centered around room temperature.[8]

$Fe(pz)[Pt(CN)_4]$ (pz = pyrazine) is another example of the SCO compound deposited and studied in the form of nanocrystalline MAPLE films. This material has been widely investigated due to its temperature hysteresis (21 K wide) occurring around room temperature, bidirectional light switching,[13] ability to detect the presence of volatile substances,[14] and sensing of pressure and temperature with optical detection.[15]

For PEG impregnated films of nanocrystalline $Fe(pz)[Pt(CN)_4]$ deposited from a mixture of the compound (0.35% wt), 1,1-dichloroethane, and polyethylene glycol, a cooperative first-order SCO transition centered at 155 K was derived from the Raman spectroscopic study. The observed downshift of the hysteresis loop to 124 K is remarkable in comparison with the reference material (hysteresis centered at 279 K) and its study is currently under continuation. As a possible explanation of this effect, the particle size reduction due to deposition, the substrate interaction,[16] and post-deposition hydration of the thin film with the latter known to produce a temperature downshifted SCO are currently considered.[17]

Interestingly, for MAPLE deposited films, a temperature downshift of SCO is also observed for the pure title compound,[18] similar to the PEG-impregnated $Fe(pz)[Pt(CN)_4]$ in contrast to the fully functional film of $RbMn[Fe(CN)_6]$. In this case, the SCO behavior of the MAPLE films is altered similar to a gradual transition curve shifted down in temperature to 170 K when compared to the cooperative transition and the 16 K wide temperature hysteresis loop around the room temperature region in the case of reference nanocrystals. The drastic loss in cooperativity within the films was ascribed to the deformation of the 3D crystalline framework with the distorted function of pyrazine linkers, at least in the laser irradiated surface regions of NP due to the laser-induced desorption.

It is worth notice that studies on MAPLE deposited SCO compounds offer an alternative route to established fabrication methods of fabrication of the thin films of organic functional materials operating around room temperature. This is confirmed in the case of $RbMn[Fe(CN)_6]$, while an unexpected degradation of the SCO behavior was observed in comparison with the starting material are observed for the $Fe(pz)[Pt(CN)_4]$ thin films. Notably, this result was obtained in studies performed under the same laser parameters and deposition conditions applied to all compounds discussed above. Therefore, the question remains open whether it originates in the deposition alone or is related to the properties of the fragile compound.

$Fe(pz)[Pt(CN)_4]$ is typically obtained in a stable dihydrated form. This material when dehydrated at 440 K and stored under vacuum at room temperature exhibits chemical stability during months. Due to its microporous structure, $Fe(pz)[Pt(CN)_4]$ is able to absorb and bond specific molecules (such as water, gases, and certain solvents) inside its framework. Studies of the absorption and desorption kinetics of H_2O, CO, or CO_2 molecules in the $Fe(pz)[Pt(CN)_4]$ crystal lattice indicate that these processes are relatively slow and their dynamics depends both on the type of molecule and environmental conditions such as partial pressure or temperature.[19] Depending on the type of bound substance, it can significantly alter SCO properties or even lock a certain spin state[14] as in the already mentioned case of increasing water concentration in the porous structure, which causes the SCO temperature downshift.[17,20] In the present study, also the theoretical stable model of pyrazine molecule bound in the crystalline structure of $Fe(pz)[Pt(CN)_4]$ is taken into account[21] and, therefore, the coupled effect of both water and pyrazine absorption cannot be excluded.

In this paper, the contribution is studied of the host–guest exchange, i.e., between pyrazine and water, to the transition temperature downshift in nanocrystalline $Fe(pz)[Pt(CN)_4]$ thin films prepared by MAPLE. The SCO properties of the deposited films are discussed in view of the laser-target energy coupling. We elucidate the effect based on experimental observation and taking into account an initial entrapment of water molecules in pores and the presence of pyrazine linkers in the crystalline framework. The laser induced host–guest exchange resulting in the stabilization of the HS state and eventually in the substantial downshift of the transition temperature in the thin film is discussed. This scenario is supported by the coincidence of the variable temperature Raman spectra and x-ray diffraction patterns.

II. EXPERIMENTAL METHODS

A. Synthesis of nanocrystalline $[Fe(pz)Pt(CN)_4]$

$Fe(BF_4)_2{\cdot}6H_2O$, $K_2[Pt(CN)_4]$, and pyrazine were obtained from Sigma-Aldrich and were used as received. Sodium bis-(2-ethylhexyl) sulfosuccinate NaAOT and octane were obtained from TCI and used without further purification. De-ionized water, used for synthesis, was deoxygenated by sonication and argon bubbling during 1 h. $Fe(pz)[Pt(CN)_4]$ nanocrystals were synthesized in water in oil microemulsions according to a method reported by Real and co-workers.[22]

B. Thin films deposition

The Fe(pz)[Pt(CN)$_4$] nanocrystalline thin films were deposited by means of a modified matrix-assisted pulsed laser evaporation (MAPLE) method using the laboratory build experimental setup consisting of vacuum chamber (K. J. Lesker) with a pressure control system and a closed-cycle He-cryostat (Leybold) with temperature control unit. The ablation process was carried out using a Nd:YAG laser Brilliant B (Quantel) operating at 1064 nm with a 10 Hz pulse repetition rate and a 6 ns pulse duration [Fig. 2(a)]. The target for the ablation process was prepared by suspending 1.2 mg of nanocrystalline Fe(pz)[Pt(CN)$_4$] powder in 0.6 ml of solvent. Two types of solvents were used: de-ionized water or acetonitrile for non-water experiments. The dispersion was solidified at cryogenic temperatures and served as the laser-ablated MAPLE target. The deposition process was carried out under vacuum conditions (10^{-6} mbar) or in nitrogen ambient at atmospheric pressure. Thin films were deposited on Si substrates heated to the temperature in the range between 293 and 323 K in order to ensure evaporation of the residual solvent. The target to substrate distance was equal to 4 and 1 cm for the deposition carried out in vacuum and at atmospheric pressure, respectively. During the ablation process, the target surface was scanned by the focused laser beam to avoid the formation of craters. The laser energy was selected from the range of 14–25 mJ, resulting in the radiation intensity at the target surface in the range of 2–3 J/cm^2. The deposition duration of a single thin film sample was in the range of 20–60 min depending on process conditions.

C. Characterization techniques

The variable temperature Raman spectra were recorded using micro-Raman spectrometer InVia (Renishaw) equipped with an LN_2 cryostat module (Oxford Instruments) and controlled by temperature controller Mercury ITC (Oxford Instruments). Raman measurements were carried out with laser excitation at 785 nm (Modu-Laser™) using laser power less than 0.1 mW. To avoid water condensation on the Fe(pz)[Pt(CN)$_4$] film during Raman measurements, samples were protected with a microscope covering glass (0.15 mm thick) and sealed in a hot press lamination process using thermoplastic 60 μm thick gasket (Surlyn, DuPont). The variable temperature Raman spectra were recorded in the range of 550–2400 cm^{-1} (resolution 1 cm^{-1}) in the temperature range of 100–320 K with 10 K steps using time intervals of 1–2 min until the temperature stabilized.

Crystalline structure was examined by x-ray diffraction (XRD) using an X'Pert Phillips diffractometer with Cu K-α radiation (1.541 Å). The diffraction patterns were analyzed with the Rietveld refinement method using the HighScore Plus software package.[23]

SEM imaging was performed using the SEM microscope FEG 250 (FEI Quanta) operated at 10 kV in a high vacuum mode.

III. RESULTS AND DISCUSSION

In accordance with the structure of the porous 3D Hoffman framework material Fe(pz)[Pt(CN)$_4$] presented in Fig. 1, the tetragonal crystalline site is formed by the bimetalic cyano-bridged 2D {Fe[Pt(CN)$_4$]} planes pillared with pyrazine ligands. The size of the crystal unit cell is determined mainly by the variable length of equatorial and axial Fe–N bonds that change with the spin state. A Fe–N bond length of 2.21 Å determined at 310 K for the HS state decreases to 1.96 Å for the LS state at 250 K and in consequence, the guest free unit cell volume decreases from 414.9 Å^3 for HS to 373 Å^3 for LS.[14,24] At the same time, the change in size induced by thermal expansion in this temperature range is negligible. Consequently, it is the spin transition that causes an essential change in the size of the channels through which guest molecules can penetrate into the porous structure of the framework.

However, in our case of the irradiation with laser pulses at nanosecond timescale that takes place during MAPLE deposition of the SCO material, the laser-induced non-equilibrium processes

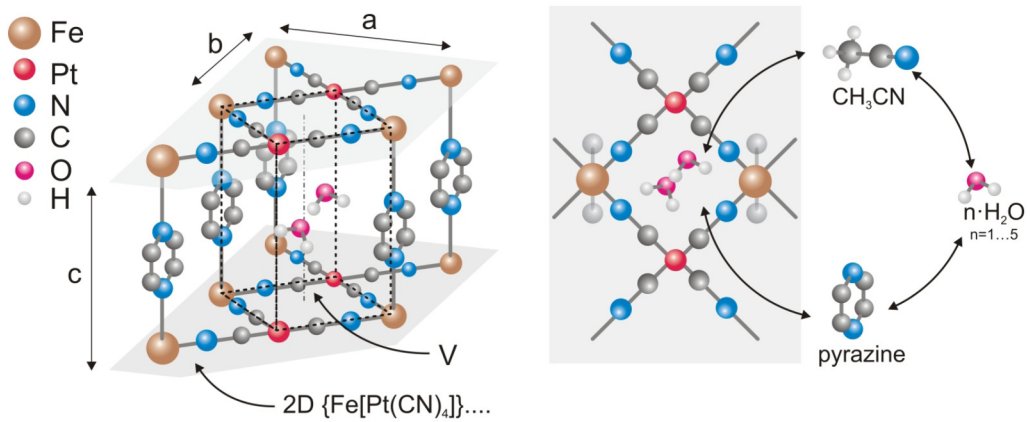

FIG. 1. Crystal structure of Fe(pz)[Pt(CN)$_4$]·2H$_2$O formed by a 2D {Fe[Pt(CN)$_4$]} planes connected with pyrazine ligands (left) and top view—perpendicular to the Fe[Pt(CN)$_4$] plane showing the Fe_2Pt_2 square windows. The volume V of the single cell cavity is usually occupied with two H_2O molecules that can be substituted with other guest molecules.

take place. These are due to the absorption of intense radiation doses that cause locally a short-term but essential increase of the crystal temperature. Moreover, laser pulses of intensity above the target ablation threshold generate shock waves resulting in vibration of the crystal lattice.

Worth to mention, calculations were carried out for conditions characterizing the MAPLE deposition process, such as energy of a single laser pulse ($E_0 = 0.02$ J), the film thickness, and geometry of laser irradiation spot, and the Fe(pz)Pt[CN]$_4$ material properties: heat capacity $c_M = 250\ \mathrm{J\ mol^{-1}\ K^{-1}}$, molar mass: $M = 435.08\ \mathrm{g\ mol^{-1}}$, density $\rho = 1.94\ \mathrm{g\ cm^{-3}}$, and molar absorption coefficient estimated as $\varepsilon = 1000\ \mathrm{mol^{-1}\ cm^{-1}}$ (basing on UV–Vis absorbance measurements). From the heat transfer equation, the value of energy delivered by the laser pulse to the film was estimated $Q = (5.8 \pm 1.4)\ \mathrm{kJ\ mol^{-1}}$ and temporary temperature increase by about 23° and also dissipation of the thermal energy due to laser pulses on the microsecond time scale were obtained. Calculations carried on using 1D heat equation for the estimation of the peak temperature on the nanocrystal particle surface due to interaction with single laser pulse resulted in values up to about 700 K.[18] The results presented below aim on the analysis of the conditions occurring during the MAPLE deposition and discussion of the possible water–pyrazine exchange process stimulated by laser irradiation in the SCO material.

A. Deposition conditions

The scheme of MAPLE thin film fabrication is presented in Fig. 2(a). For deposition, the nanocrystalline material is dispersed in the solvent (matrix) and after solidification on the cryostat head serves as a target for laser ablation. The fundamental radiation of Nd:YAG laser (1064 nm) is selected for ablation because this wavelength is relatively distant from Fe(pz)[Pt(CN)$_4$] absorption bands. Simultaneously, this wavelength corresponds to higher vibration overtones of O–H, C–H, and N–H bonds of water and most organic solvents, resulting in increased absorbance; however, the matrix absorbance in this spectral range is still relatively low. Therefore, laser can penetrate the target to a certain depth, causing volumetric ablation and result in the micro-spray ejection of partial only evaporated solvent mixed with nanoparticles as shown in Fig. 2(b). The propagation and spatial distribution of the ablated material are determined mainly by ambient gas pressure. In vacuum or in low pressure conditions, the ablated species do not interact or interact only weakly with ambient gas, and the evaporated solvent is efficiently evacuated with vacuum pump. Conversely, higher pressure values cause the reduction of the propagation speed due to collisions of the ablated material with ambient gas. Simultaneously, also the solvent evaporation rate is limited what can result in microdroplets consisting not only of the material to be deposited but also of the solvent reaching the substrate surface. The effect of main parameters of the deposition process such as the ambience (vacuum or an inert gas, the laser wavelength, fluence, and pulse rate) on spin crossover properties of the Fe(pz)[Pt(CN)$_4$] nanocrystalline film is discussed further in Secs III B–III D.

B. Vacuum deposited films

Since a stream of laser ablated material can be highly decelerated due to interaction with ambient gas, the laser assisted deposition processes such as PLD or MAPLE are conducted predominantly in vacuum or in an inert/processing gas at low pressure. In our case, the target was prepared using water suspension of SCO nanocrystals rapidly solidified at 80 K on the cryostat head. The nanocrystalline Fe(pz)[Pt(CN)$_4$] film was deposited in vacuum conditions (10^{-6} mbar) and the target–substrate distance was equal to $d = 40$ mm. After 60 min of deposition, the silicon substrate was covered with a thin, irregular film of nanocrystals. Structure and properties of the deposited material were analyzed by means of a variable temperature Raman spectroscopy [Fig. 3]. Raman spectra exhibit CN stretching modes around 2200 cm^{-1} and pyrazine internal modes between 600 and 1600 cm^{-1}. The lower frequency modes can be attributed primarily to metal–ligand vibrations and lattice phonons. Several vibrational modes may be followed to probe the change in the spin state: the pyrazine in-plane bending mode,[5] which exhibits a shift from 643 to 656 cm^{-1} when going from the high-spin (HS) to the low-spin (LS) state or the more intense bands centered at 1030 and 1233 cm^{-1}.

Raman spectra presented in Figs. 3(a) and 3(b) were recorded for MAPLE deposited thin film, while spectra presented in Figs. 3(c) and 3(d) for the reference nanocrystalline Fe(pz)[Pt(CN)$_4$] powder,

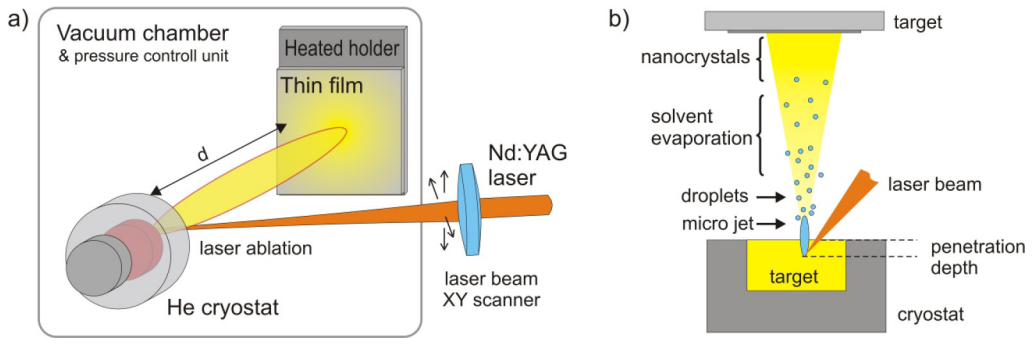

FIG. 2. Scheme of the experimental setup (a) and the laser-induced deposition mechanism (b).

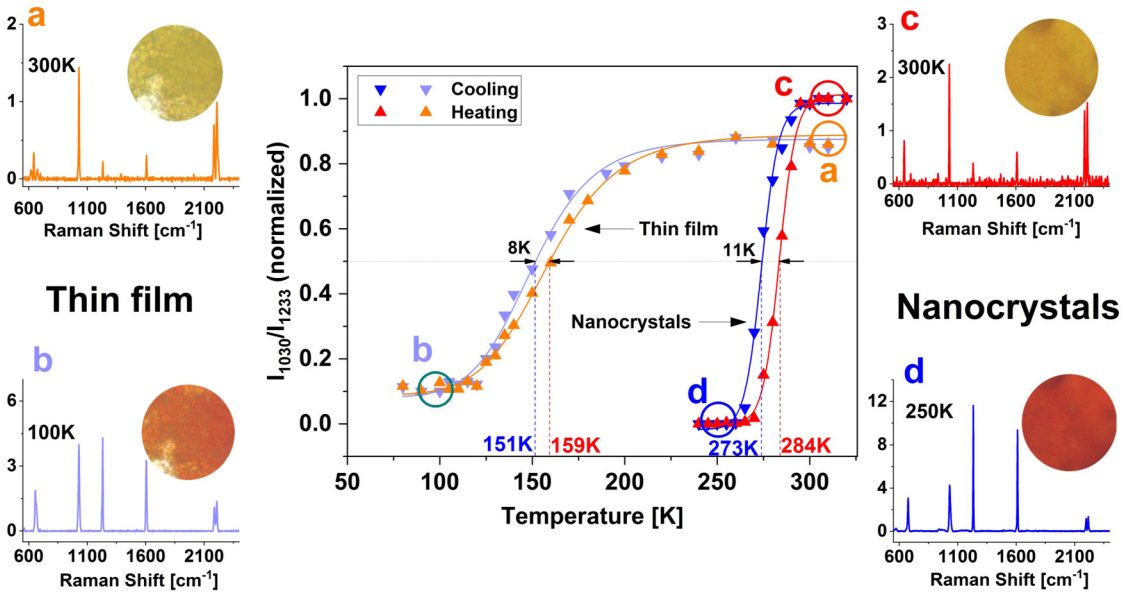

FIG. 3. Raman spectra recorded for the MAPLE deposited thin film [(a) and (b)] and nanocrystalline Fe(pz)[Pt(CN)$_4$] powder [(c) and (d)] in the HS (320 K) and LS (110 and 250 K, respectively) states; the central graph shows temperature dependence of the normalized Raman intensity ratio [I(norm) = I(1030 cm^{-1})/I(1233 cm^{-1})] for the nanopowder and thin film samples upon cooling (down triangles) and heating (up triangles) and presents the thermally induced spin transition.

both in the HS and LS spin states, respectively. The temperature dependent characteristics presented in the central part of Fig. 3 correspond to the spin state determined on the basis of Raman bands centered at 1030 cm^{-1} and 1233 cm^{-1}. The spectra of the reference material and thin film samples are virtually identical. Moreover, in both samples, the frequency shifts in the region around 660 cm^{-1} that correspond to the thermally induced spin crossover can be observed. Although the Raman spectra do not reveal changes in the structure of the deposited SCO material, the temperature dependent Raman characteristics indicate a significant reduction of the spin transition temperature in the case of the thin film. While the spin transition in the film is preserved what follows from Raman spectra and is confirmed by the observed color changes of the sample, a decrease in switching temperature by 130 K down to 150 K region is observed. The hysteresis narrowed to 8 K of the laser-deposited film differs not substantially from the 11 K wide hysteresis loop of the raw reference material. A similar significant change in the spin transition temperature down to 180 K has been reported in our previous paper for samples prepared with the use of water matrix under comparable conditions.[18] Worth to notice are two observations, namely, both the loop width and range of transition temperatures of the starting material when compared with values reported for this completely dehydrated compound could indicate the presence of H_2O in the porous NP structure. As mentioned, the compound is typically found in its dihydrate form Fe(pz)[Pt(CN)$_4$]·2H_2O of stability supported by the results of model simulation. The simulated dependence of transition temperature vs number of water molecules per clathrate calculated for Fe(pz)[Pt(CN)$_4$] is presented in Fig. 4.[21] The number n of water molecules can change from n = 0 to 5. Numerical simulations show that for the water free structure, the spin transition temperature is approximately 300 K and decrease slightly to 280 K if one or two water molecules are absorbed in MOF clathrate what is observed experimentally for dihydrate form

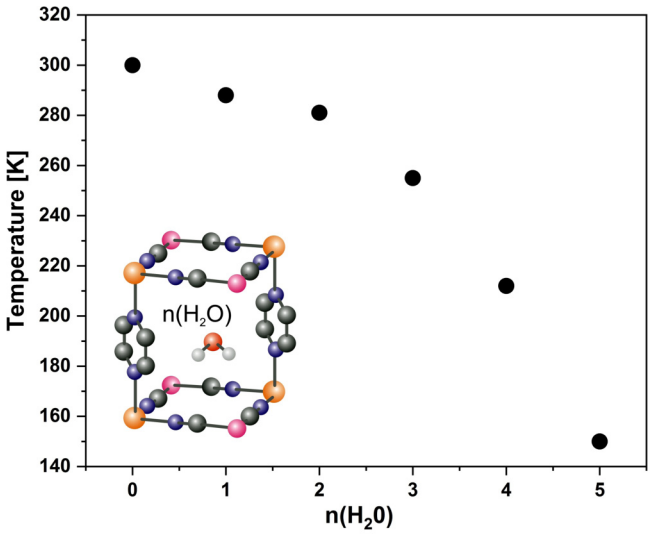

FIG. 4. Spin transition temperature T1/2 dependence on the number of water molecules inside the unit cell of Fe(pz)[Pt(CN)$_4$]; results of numerical modeling adapted from Ref. 21.

$Fe(pz)[Pt(CN)_4]\cdot 2H_2O$. If the number of water increase above two molecules per clathrate significantly, the decrease of spin crossover temperature is observed. This phenomenon can be directly related to the elongation of the Fe–N bond distance for the water saturated crystalline MOF structure in its low spin state, what leads to stabilization of HS.[21]

In our case, for the temperature downshifted to 150 K, the model would predict a full saturation of the unit cell with water molecules what cannot be accepted in view of experimental conditions (vacuum deposition) where desorption of guest molecules is preferred. This observation indicates on the another important factor which is related to laser radiation. More precisely, it is the pressure and thermal shock induced by the laser pulse, which both can lead to the laser driven desorption of guest molecules in the porous structure and also to dynamic deformations of the SCO crystalline network what eventually results in substantial degradation of the cooperativity.[19,25,26]

C. Films fabricated in N_2 at elevated pressure

In order to eliminate or at least minimize the negative influence of the sorption–desorption effect due to vacuum during laser ablation on the spin transition characteristics, the deposition experiment has been repeated at atmospheric pressure. The target was prepared using an identical procedure. In addition to the de-ionized water target, an alternative water free target was prepared using the organic solvent acetonitrile. During the deposition, the processing chamber was filled with nitrogen under atmospheric pressure. Due to the strong deceleration of ablated material as a result of collision with surrounding gas, the target to the substrate distance has been reduced from d = 40 to d = 10 mm. The laser parameters such as energy density, wavelength, and repetition rate were identical as in the previous experiment.

The temperature dependent spin crossover characteristics of thin films deposited with the use of water and acetonitrile targets are presented in Fig. 5. In the case of sample deposited from water based matrix at atmospheric pressure, only a slight temperature decrease down to $T_{tr} = 271$ K is observed compared to the reference material ($T_{tr} = 279$ K) and can be attributed to the inconsiderable increase of water amount in the SCO film (or a slight structural damage). In the case of the sample prepared at atmospheric pressure using water-free acetonitrile based matrix, the spin crossover temperature experiences a downshift to 236 K, i.e., observably stronger than in the case of water matrix. This can be explained with diffusion of acetonitrile molecules into pores of the $Fe(pz)[Pt(CN)_4]$ crystal network that stabilize HS state more effectively than water.[2,18] Of course, this water–acetonitrile exchange is possible under the assumption that water molecules have been completely or in part removed from pores of the framework during its short term expansions induced by laser pulses. As already mentioned in Sec. III A, Nd:YAG laser radiation at 1064 nm is relatively poorly absorbed in the solvent served as a matrix, as a result of which a significant amount of the laser radiation is absorbed by the nanocrystalline MOF material suspended in the matrix. Intensive laser radiation causes a temporary increase in the temperature of the crystal and vibrations of the crystal lattice, which may lead to the ejection of water molecules from the pores of the crystal lattice.

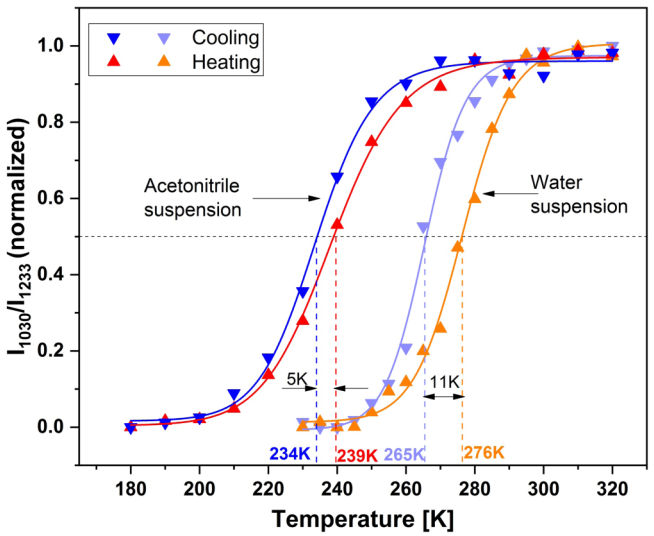

FIG. 5. Temperature dependence of spin transition for thin films deposited with use of targets prepared from water and acetonitrile suspensions, both films were deposited at atmospheric pressure.

The high concentration of solvent vapors generated by laser ablation promotes the penetration of solvent molecules into the porous crystal structure.[10] In the case of the water based matrix, the lack of the effect of the penetration of additional water molecules into the crystal structure may be due to the fact that the preferred and most stable is the structure containing two molecules per clathrate.

Nevertheless, both results observed for water and acetonitrile indicate that for guest molecules stabilizing the HS state, the spin transition temperature of the SCO material is a function of the number of guest molecules. However, quantitative analysis of the laser induced exchange of guest molecules represents a difficult task due to transient processes at nanosecond time scale and non-equilibrium heat exchange and also framework relaxation during microseconds after laser pulses.[21]

D. Raman and XRD signatures due to laser irradiation

In order to explain the processes induced by laser irradiation of nanocrystalline $Fe(pz)[Pt(CN)_4]$ under typical deposition conditions, it was advisable to complement the study with Raman and XRD measurements performed on samples with disentangled influence of the solvent (matrix). Prior laser irradiation the nanocrystalline powder of SCO material was trapped between two glass plates (0.15 mm microscope slide glass) to avoid its atomization due to laser induced shockwave. The raw material (reference sample) was irradiated using laser parameters comparable to these applied during the MAPLE process, while the irradiation was conducted once in N_2 under atmospheric pressure and in the second case, in vacuum ($<10^{-3}$ mbar). Each sample was treated with at least 20 laser pulses. Immediately after laser processing, the SCO material was analyzed by means of micro-Raman as well as x-ray diffraction techniques. Raman spectra in Fig. 6 registered at room temperature

for samples irradiated in N_2 at atmospheric pressure [Fig. 6(b)] and in vacuum [Fig. 6(c)] do not indicate any marked changes compared to the non-irradiated reference sample [Fig. 6(a)]. Also, the comparison of SEM images of the reference and laser irradiated samples (Fig. 6, right panel insets) do not evidence any visible modification of the size and shape of nanocrystals. Basing on the temperature dependent Raman measurements, the spin transition characteristics were determined from changes of the relative intensity of Raman bands centered at 1030 and 1233 cm^{-1} (Fig. 6 right panel). For the sample irradiated with laser under ambient pressure, very similar spin transition characteristics with reproduced hysteresis loop is observed in comparison to the reference nanomaterial. In contrary, the sample irradiated in vacuum shows a substantial decrease of the transition temperature. Because of negligible only differences in the material structure can be observed in the Raman study supported by SEM inspection, it can be concluded that the effect observed for sample irradiated in vacuum and the associated downshift in spin transition temperature is most likely related to the formation of clathrates containing guest molecules what agrees with results in Secs. III B and III C.

In order to provide complementary results for explanation of the spin transition characteristics exhibited by the laser irradiated sample in vacuum, the x-ray diffraction patterns were registered for that sample and the reference one [Fig. 7]. From the pattern similarity of the latter that reproduces main reflexes present in the reference pattern, it could be concluded that laser does not affect the crystalline structure of the material framework. However, for the sample irradiated with laser in vacuum additional peaks can be observed at $2\Theta = 11.8°$, 17.1°, 30.5°, and 31.0°, which can be assigned to $Fe(pz)[Pt(CN)_4]$ enriched by pyrazine molecules trapped as a guest.[14] This could result from partial release of pyrazine molecules in the framework structure, specifically in the outer nanoparticle regions exposed to intense laser radiation. Released molecules can be bound inside unit cells and form the pyrazine containing clathrates that lower the spin switching temperature as it was proposed by Pham and Paesani.[27] At the same time, the pyrazine relocation

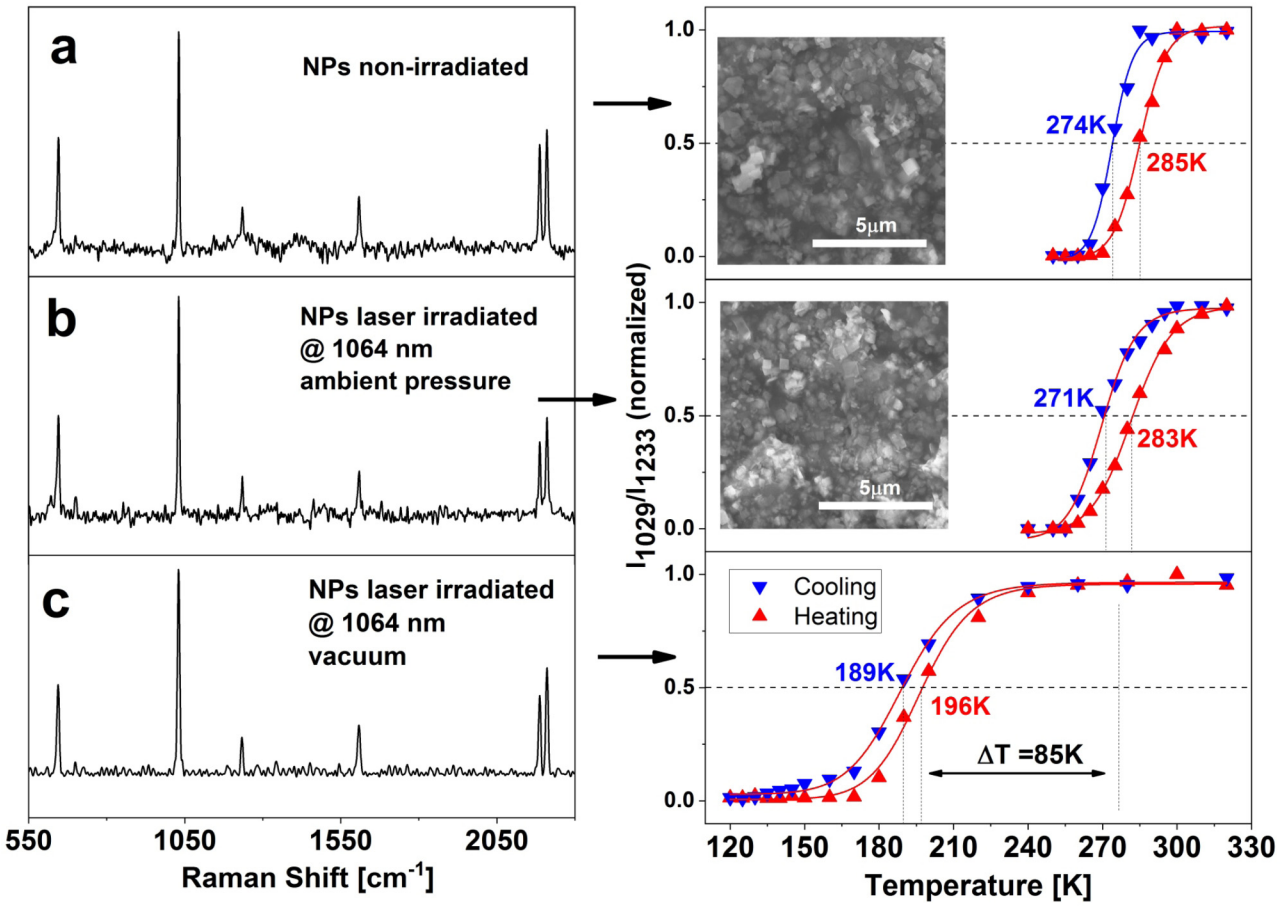

FIG. 6. Raman spectra registered at room temperature for the $Fe(pz)[Pt(CN)_4]$ nanopowder—reference (a) and for samples of the same nanopowder irradiated at atmospheric pressure (b) and in vacuum (c); right panel shows the corresponding temperature dependences of spin transition characteristics and SEM images of the sample surfaces (insets).

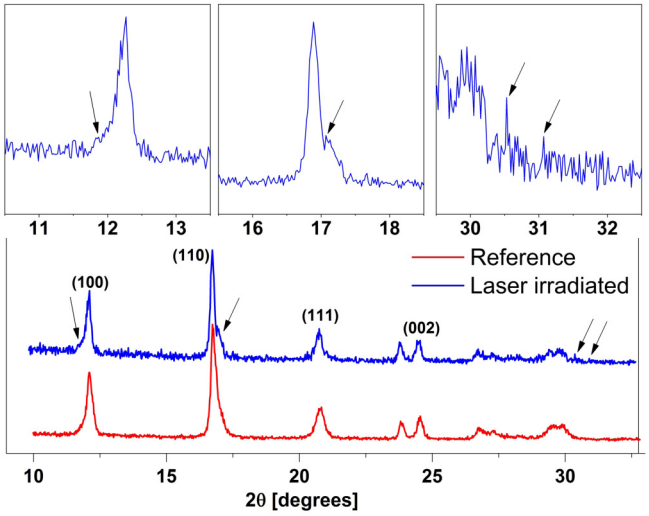

FIG. 7. XRD patterns of a reference nanopowder Fe(pz)[Pt(CN)$_4$] and the sample irradiated with laser in vacuum. Arrows indicate reflexes at 2Θ = 11.8°, 17.1°, 30.5°, and 31.0°, which can be assigned to Fe(pz)[Pt(CN)$_4$] pyrazine clathrates.

changes locally the structure of the crystalline material. The resulting deformation disrupts cooperativity and eventually locks the HS state of the surrounding molecules. Recently, a similar effect resulting from dynamic structural transformation due to chemisorption of dehydrated Fe(pz)[Pt(CN)$_4$] with water and piridyne coordinating to the open Fe^{2+} site was reported.[28]

IV. CONCLUSIONS

This work aimed at elucidating the mechanism of the host–guest exchange contribution to transition temperature downshift in nanocrystalline Fe(pz)[Pt(CN)$_4$] thin films prepared by matrix-assisted pulsed laser evaporation. Therefore, the characteristics of the spin transition of films deposited with water and water-free solvents used as matrices were studied using the Raman and XRD spectroscopy and SEM imaging. For assessment of the sorption effect due to vacuum on the deposited material, additional measurements were performed in inert gas (N_2) at atmospheric pressure. The results indicate several factors able to affect negatively the spin transition.

First, the use of a laser wavelength in the near infrared range (1064 nm) to induce the deposition creates specific conditions in which ablation and evaporation of the target take place. At the same time, the SCO material is exposed to the laser radiation pulses, which cause thermal shock and vibration of the crystal lattice. Given the required deposition conditions, most of the energy delivered by laser pulses at this wavelength is absorbed by the evaporating matrix. Despite low concentration of the fragile SCO compound, it absorbs a residual part of the radiation energy what stimulates molecular rearrangements in the framework and can result in a substantial loss of cooperativity due to framework destruction and collapse or in the host–guest exchange, e.g., between structural water and pyrazine rings. The possibility of the latter scenario is supported by the fact that thin films deposited under vacuum exhibit the spin transition temperature significantly decreased (150 K) in comparison to 273 K measured for the reference material. Consequently, while Raman spectra of vacuum irradiated nanoparticles show transition temperature decreased to 193 K and do not reveal any changes in the molecular structure, the XRD patterns indicate the presence of reflexes that can be ascribed to pyrazine. This implies that laser impact on the framework can be responsible not only for desorption of the structural water but also for a decrease of the material cooperativity due to its partial destruction and displacement of the pyrazine rings. The latter when released from their pillar positions in the crystal lattice become guest molecules that eventually stabilize the HS state.

In the case of film deposition in an inert gas at atmospheric pressure, the laser stimulated exchange between water molecules forming originally the dihydrate crystal lattice and the solvent molecules released from the target during ablation is postulated as responsible for the observed change in spin transition. This follows from the observed nearly unchanged spin transition in the case of water based matrix (target) with spin crossover temperature at 271 K hysteresis loop width of 12 K, while in the case of water-free matrix (acetonitrile), the desorbed water is replaced with guest molecules that form clathrates. The acetonitrile guest molecules are known to stabilize the HS state what results in the downshift of the spin crossover temperature to 236 K. This laser-stimulated host–guest exchange indicates on the useful possibility of selective modification of thin layers of SCO materials to obtain desired characteristics of novel sensing devices.

ACKNOWLEDGMENTS

The authors acknowledge financial support from the FNRS-PAN (No. CDR 33694457) and WBI-MNiSW (No. CDR 33694457) joint research projects, Fonds De La Recherche Scientifique—FNRS (No. PDR T.0095.21), and D.M. funding via project No. 2018/31/N/ST8/01797 of the National Research Council (NCN) of Poland. Also, collaboration in the frame of the COST Action CA17123 is appreciated.

DATA AVAILABILITY

The data that support the findings of this study are available from the corresponding author upon reasonable request.

REFERENCES

[1]M. Ruben and K. S. Kumar, Angew. Chem. Int. Ed. **60**, 7502 (2021).
[2]V. Niel, J. M. Martinez-Agudo, M. C. Muñoz, A. B. Gaspar, and J. A. Real, Inorg. Chem. **40**, 3838–3839 (2001).
[3]M. Cavallini, Phys. Chem. Chem. Phys. **14**, 11867 (2012).
[4]G. Molnár, S. Rat, L. Salmon, W. Nicolazzi, and A. Bousseksou, Adv. Mater. **30**, 1703862 (2018).
[5]S. Cobo, G. Molnár, J. A. Real, and A. Bousseksou, Angew. Chem. Int. Ed. **45**, 5786 (2006).
[6]K. Otsubo, T. Haraguchi, and H. Kitagawa, Coord. Chem. Rev. **346**, 123 (2017).
[7]V. Shalabaeva, S. Rat, M. D. Manrique-Juarez, A.-C. Bas, L. Vendier, L. Salmon, G. Molnár, and A. Bousseksou, J. Mater. Chem. C **5**, 4419 (2017).

[8]D. Maskowicz, M. Sawczak, R. Jendrzejewski, M. Gazda, H. Tokoro, S. Ohkoshi, Y. Garcia, and G. Śliwiński, Scr. Mater. **183**, 50 (2020).
[9]M. Sawczak, R. Jendrzejewski, D. Maskowicz, Y. Garcia, A. C. Ghosh, M. Gazda, J. Czechowski, and G. Śliwiński, Eur. J. Inorg. Chem. **2019**, 3249 (2019).
[10]A. D. Stiff-Roberts and W. Ge, Appl. Phys. Rev. **4**, 041303 (2017).
[11]A. P. Caricato, M. Cesaria, C. Leo, M. Mazzeo, A. Genco, S. Carallo, T. Tunno, A. Massafra, G. Gigli, and M. Martino, J. Phys. D: Appl. Phys. **48**, 135501 (2015).
[12]H. Tokoro, T. Matsuda, T. Nuida, Y. Moritomo, K. Ohoyama, E. D. L. Dangui, K. Boukheddaden, and S. Ohkoshi, Chem. Mater. **20**, 423 (2008).
[13]S. Cobo, D. Ostrovskii, S. Bonhommeau, L. Vendier, G. Molnár, L. Salmon, K. Tanaka, and A. Bousseksou, J. Am. Chem. Soc. **130**, 9019 (2008).
[14]M. Ohba, K. Yoneda, G. Agustí, M. C. Muñoz, A. B. Gaspar, J. A. Real, M. Yamasaki, H. Ando, Y. Nakao, S. Sakaki, and S. Kitagawa, Angew. Chem. Int. Ed. **48**, 4767 (2009).
[15]J. Linares, E. Codjovi, and Y. Garcia, Sensors **12**, 4479 (2012).
[16]T. Delgado, C. Enachescu, A. Tissot, L. Guénée, A. Hauser, and C. Besnard, Phys. Chem. Chem. Phys. **20**, 12493 (2018).
[17]S. Bonhommeau, G. Molnár, A. Galet, A. Zwick, J.-A. Real, J. J. McGarvey, and A. Bousseksou, Angew. Chem. Int. Ed. **44**, 4069 (2005).
[18]D. Maskowicz, M. Sawczak, A. C. Ghosh, K. Grochowska, R. Jendrzejewski, A. Rotaru, Y. Garcia, and G. Śliwiński, Appl. Surf. Sci. **541**, 148419 (2021).
[19]D. Alvarado-Alvarado, J. H. González-Estefan, J. G. Flores, J. R. Álvarez, J. Aguilar-Pliego, A. Islas-Jácome, G. Chastanet, E. González-Zamora, H. A. Lara-García, B. Alcántar-Vázquez, M. Gonidec, and I. A. Ibarra, Organometallics **39**, 949 (2020).
[20]A. Holovchenko, J. Dugay, M. Giménez-Marqués, R. Torres-Cavanillas, E. Coronado, and H. S. J. van der Zant, Adv. Mater. **28**, 7228 (2016).
[21]C. H. Pham, J. Cirera, and F. Paesani, J. Am. Chem. Soc. **138**, 6123 (2016).
[22]I. Boldog, A. B. Gaspar, V. Martínez, P. Pardo-Ibañez, V. Ksenofontov, A. Bhattacharjee, P. Gütlich, and J. A. Real, Angew. Chem. Int. Ed. Engl. **47**, 6433 (2008).
[23]T. Degen, M. Sadki, E. Bron, U. König, and G. Nénert, Powder Diffr. **29**, S13 (2014).
[24]E. Collet, L. Henry, L. Piñeiro-López, and J. A. Real, Curr. Inorg. Chem. **6**, 61 (2016).
[25]T. Delgado, A. Tissot, C. Besnard, L. Guénée, P. Pattison, and A. Hauser, Chem. Eur. J. **21**, 3664 (2015).
[26]A. Muraoka, K. Boukheddaden, J. Linarès, and F. Varret, Phys. Rev. B **84**, 54119 (2011).
[27]C. H. Pham and F. Paesani, J. Phys. Chem. Lett. **7**, 4022 (2016).
[28]T. Haraguchi, K. Otsubo, O. Sakata, A. Fujiwara, and H. Kitagawa, J. Am. Chem. Soc. **138**, 16787 (2016).